Response dynamics of an alkali-metal–noble-gas hybrid trispin system

Guobin Liu [1,2,*] Vera Guarrera,[3] Sihong Gu,[4,2] and Shougang Zhang[1,2]

[1]*National Time Service Center, Chinese Academy of Sciences, Xi'an 710600, China*
[2]*University of Chinese Academy of Sciences, Beijing 100049, China*
[3]*School of Physics and Astronomy, University of Birmingham, Edgbaston, Birmingham B15 2TT, United Kingdom*
[4]*Innovation Academy for Precision Measurement Science and Technology, Chinese Academy of Sciences, Wuhan 430071, China*

We study the dynamics of a comagnetometer based on an alkali-metal—noble-gas hybrid tri-spin system by numerically solving coupled Bloch equations. A thorough analysis of the response dynamics is carried out in the standard experimental regime where the spin system can be mapped to a damped harmonic oscillator. The results show that a linear increasing response of the comagnetometer signal is found when the noble-gas nuclear spin magnetization and the alkali-metal spin lifetime parameters satisfy an overdamping condition. We find that an upper limit for the signal amplitude of the comagnetometer is imposed by the inherent dynamics of the hybrid tri-spin system. The results agree with currently available experimental data and provide useful guiding for future experiments.

The nuclear spins of noble gases can be easily polarized to a high degree by spin-exchange optical pumping [1]. Once polarized, nuclear spins can be hardly disturbed by the ambient static or electromagnetic fields due to their full shell electron configuration. These features make the nuclear spin polarization of noble gases a perfect resource for various scientific and practical purposes. As an example, trispin comagnetometers using one alkali-metal and two noble-gas species have recently become attractive for potential applications in the fundamental physics measurement [2,3], and as a nuclear magnetic resonance (NMR) gyroscope for inertial navigation [4,5] due to their exceptional sensing performances.

The basic principle of these comagnetometers is to let the nuclear spin polarizations precess around a static magnetic field and then read these precessions out by using an alkali-metal gas, which occupies the same volume of the noble-gases' spins as an ultrasensitive *in situ* magnetometer. Besides the polarization preparation and the magnetometer readout process, this hybrid trispin dynamic system itself displays a rich physical scenario deserving comprehensive study. The alkali-metal–noble-gas dual spin system has already revealed interesting nonlinear dynamics near the zero magnetic field as shown both experimentally and theoretically for the K-^{3}He system [6]. However, a similar thorough analysis for trispin systems, such as Rb-^{3}He-^{129}Xe [3] and Rb-^{129}Xe-^{131}Xe [7] is still unavailable now.

Recently we have studied the trispin dynamics by using numerical simulations of the coupled Bloch equations [8]. Empirical formulas were derived for the multiple-peak structure of the NMR spectra in the partial coupling configuration of the trispin system. Here, we would like to further extend the study of the trispin dynamics to disclose more information crucial for the operation of ultrasensitive trispin comagnetometers.

We assume a classical macroscopic magnetization field **M** is created for both the alkali vapor and the noble gases by mixed spin-exchange and optical pumping. Two basic interaction processes dominate the spin magnetization dynamics of the trispin system: the spin-field interaction between the atomic spin magnetizations, the static bias magnetic-field **B**$_0$, and the spin-spin interaction between the alkali spin magnetization and the spin magnetizations of the noble gases.

The first interaction is well described by classical Bloch equations. Concerning spin-spin interactions, they have been shown to shift both the frequency of electron-paramagnetic-resonance lines of alkali-metal atoms, and the NMR lines of noble-gas atoms [9]. These frequency shifts can be represented by introducing an effective spin-exchange field **B**$_{se}$, which can be expressed as

$$\mathbf{B_{se}} = \lambda \mathbf{M} = \frac{8\pi}{3}\kappa_0 \mathbf{M}. \tag{1}$$

This spin-exchange field is enhanced by a coefficient λ in comparison to the classical macroscopic magnetization due to the attractive force between the alkali atomic valence electron and the noble-gas nucleus. The enhancement factor κ_0 is determined by the degree of overlap between the valence electron of the alkali atom and the noble-gas nucleus [9]. It also depends weakly on the rate of spin-exchange collisions, and, thus, on the temperature of the gases [10].

Following the approach used in Ref. [6], the linear coupled Bloch equations of the trispin system read

$$\dot{\mathbf{M}}^e = \frac{\gamma_e}{q}\mathbf{M}^e \times [\mathbf{B}_0 + \lambda_1 \mathbf{M}^{n_1} + \lambda_2 \mathbf{M}^{n_2}] + \frac{M_0^e \hat{z} - \mathbf{M}^e}{qT^e},$$

$$\dot{\mathbf{M}}^{n_1} = \gamma_1 \mathbf{M}^{n_1} \times [\mathbf{B}_0 + \lambda_1 \mathbf{M}^e + \lambda_3 \mathbf{M}^{n_2}] + \frac{M_0^{n_1}\hat{z} - \mathbf{M}^{n_1}}{[T_2^{n_1}, T_2^{n_1}, T_1^{n_1}]},$$

$$\dot{\mathbf{M}}^{n_2} = \gamma_2 \mathbf{M}^{n_2} \times [\mathbf{B}_0 + \lambda_2 \mathbf{M}^e + \lambda_3 \mathbf{M}^{n_1}] + \frac{M_0^{n_2}\hat{z} - \mathbf{M}^{n_2}}{[T_2^{n_2}, T_2^{n_2}, T_1^{n_2}]}.$$

$$\tag{2}$$

---
*liuguobin@ntsc.ac.cn

Here, the e in the subscript and superscript stands for the collective alkali atomic spin, which is mainly contributed by the outmost valence electron spin. n_1 and n_2 refer to the nuclear spins of the noble-gas species 1 and 2, respectively. T_1 and T_2 are the longitudinal and transverse spin-relaxation times for the corresponding spin species as indicated by the superscript. M_0 is the initial spin magnetization, and q is the slowing-down factor due to nuclear angular momentum [11]. Regarding the choice of the initial conditions, the nuclear spin magnetization has to be orthogonal to the direction of the bias magnetic-field ($\mathbf{B}_0$, along the z axis) in order to acquire a nonzero torque from the bias field. Without loss of generality and for convenience, we let alkali atomic spin magnetization lie along the x direction and nuclear spin magnetization along the y direction.

Previously, we have theoretically shown that alkali-metal–noble-gas spin decoupling is necessary to realize precision comagnetometer without frequency shifts [8]. In practice, this can be performed by modulating the alkali spins with an electro-optical modulator, by periodic optical pumping [7], or by using NMR pulse decoupling techniques [3]. Indeed, in the presence of fast periodic modulations of the alkali spins, their precession around the dc bias field and the precession of the nuclear spins around the alkali spin magnetization, are both effectively averaged out, leaving the alkali macroscopic spin sensitive only to the nuclear spin magnetization. In this case, the Bloch equations take the form

$$\dot{\mathbf{M}}^e = \frac{\gamma_e}{q}\mathbf{M}^e \times [\lambda_1\mathbf{M}^{n_1} + \lambda_2\mathbf{M}^{n_2}] + \frac{M_0^e\hat{z} - \mathbf{M}^e}{qT^e},$$

$$\dot{\mathbf{M}}^{n_1} = \gamma_1\mathbf{M}^{n_1} \times [\mathbf{B}_0 + \lambda_3\mathbf{M}^{n_2}] + \frac{M_0^{n_1}\hat{z} - \mathbf{M}^{n_1}}{[T_2^{n_1}, T_2^{n_1}, T_1^{n_1}]},$$

$$\dot{\mathbf{M}}^{n_2} = \gamma_2\mathbf{M}^{n_2} \times [\mathbf{B}_0 + \lambda_3\mathbf{M}^{n_1}] + \frac{M_0^{n_2}\hat{z} - \mathbf{M}^{n_2}}{[T_2^{n_2}, T_2^{n_2}, T_1^{n_2}]}. \quad (3)$$

At this point we can map the trispin system (and its dynamics) to a harmonic oscillator, based on the following experimental facts:

(1) once polarized and without significant interference, the noble-gas nuclear spins can keep their polarization for tens of seconds or even longer (e.g., hours for the ^{3}He spin). In comparison, the alkali atomic spin polarization is short lived, typically decaying in 1–100 ms, and very sensitive to the ambient conditions, such as temperature and buffer gas pressure. In most cases the condition $T^n \geqslant 10^4 T^e$ holds;

(2) with a heavier particle mass, the nuclear spin carries a smaller magnetic moment than the electron spin, determining a weaker spin-field interaction with the magnetic field and a smaller gyromagnetic ratio. Specifically for the case of interest for this paper, the nuclear spin gyromagnetic ratio is typically about 10^3 times smaller than that of the electron spin, i.e., ~1 MHz/G versus ~1 kHz/G.

Therefore, we can consider the nuclear spin motion as a sinusoidally varying driving force and the alkali atomic spin motion as a damped harmonic oscillator. Although the damping effect of the nuclear harmonic oscillators can be neglected due to their long spin lifetime, the alkali atomic spin oscillator has a significant damping rate, i.e., the inverse of its lifetime $\gamma = 2\pi/qT^e$. The natural frequency of the alkali atomic spin
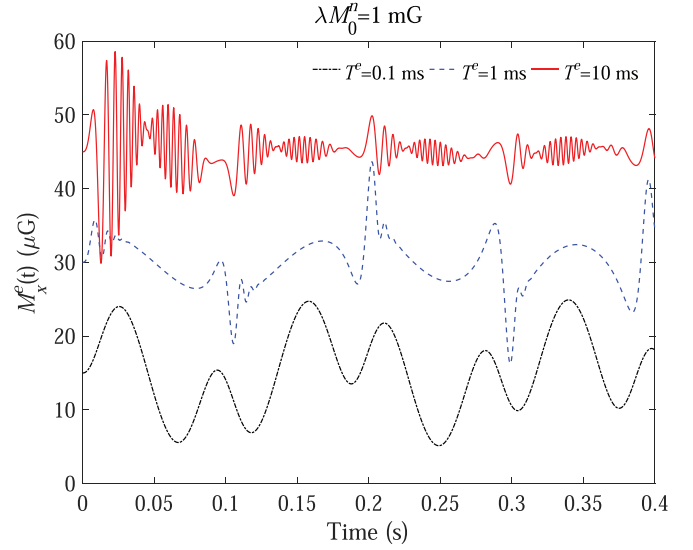

FIG. 1. Time evolution of the alkali atomic transverse spin magnetization $M_x^e(t)$ calculated for different spin lifetimes T^e. The electron spin oscillation is seen as a damped harmonic oscillator with the critical damping condition determined by $\lambda\mathbf{M}^\mathbf{n}T^e = 2\pi/\gamma_e$. As T^e increases, the alkali atomic spin oscillation moves from overdamping to underdamping, corresponding to an adiabatic and nonadiabatic following of alkali atomic spin to noble-gas nuclear spin, respectively. The T_1 and T_2 spin-relaxation times are taken 1 h and 1000 s for ^{3}He, 1000 s and 80 s for ^{129}Xe. The enhancement factor κ_0 is taken as 5, 500, and -0.011 for Rb-He [10], Rb-Xe [12], and He-Xe [13,14] spin-exchange interactions, respectively.

oscillator is the Larmor frequency, i.e., $\omega_0 = \gamma_e\lambda M^n/q$, which depends on the amplitude of the nuclear spin magnetization M^n. In this picture, the critical point between under- and overdamping of the alkali atomic spin oscillation is found for $\omega_0 = \gamma$, which gives the condition,

$$\lambda\mathbf{M}^nT^e = 2\pi/\gamma_e. \quad (4)$$

As a demonstration of this critical damping mechanism, we show the results obtained by numerically solving Eqs. (3). Figure 1 shows the initial 0.4 s of oscillation of the transverse alkali atomic spin magnetization for different values of the spin lifetime. These simulations have been performed for ^{87}Rb with $\gamma_e = 2\pi \times 0.7$ MHz/G with critical point $\lambda\mathbf{M}^\mathbf{n}T^e = 2\pi/\gamma_e \approx 1.43$ mG ms.

In Fig. 1, it can be seen that for $\lambda M_0^n T^e = 10$ mG ms > 1.43 mG ms, e.g., with $T^e = 10$ ms, the alkali atomic spin oscillation is underdamped. Indeed one can observe a fast oscillation at the damped frequency $\omega_1 = \sqrt{\omega_0^2 - \gamma^2}$. Note that as $\mathbf{M}^n$ is a sinusoidal function of time, ω_1 is also dynamically changing. For $\lambda M_0^n T^e = 0.1$ mG ms < 1.43 mG ms, e.g., with $T^e = 0.1$ ms, the alkali atomic spin oscillation is instead overdamped, and it adiabatically and smoothly follows the slow precession of the nuclear spin oscillations. Finally, when $\lambda M_0^n T^e \simeq 1$ mG ms with $T^e = 1$ ms, the alkali atomic spin magnetization oscillates at a much smaller frequency and is shortly damped to its quasisteady state, which is completely determined by the nuclear spin precession.

Even though the long coherence time of the noble-gas nuclear spin has been longly referred to as an advantage for atomic comagnetometer and NMR gyroscopes, the underlying mechanism of the coherence transfer between the different species of spins is not trivial. Here, our analysis of the critical damping mechanism provides a convenient way of understanding it. We also note that compared to other coherence transfer mechanisms in different spin systems [15,16], this coherence transfer naturally occurs with properly set parameters of the hybrid spin system, which can be easily manipulated [17].

It is interesting to note that in pure alkali spin magnetometry, longer atomic coherence lifetimes lead to better sensitivity for the magnetic-field detection. However, in a hybrid trispin comagnetometer, a strong damping factor, which means a short alkali atomic spin lifetime, is needed to realize a good coherence transfer from the noble-gas nuclear spin to the alkali atomic spin during their coupled evolution.

More precisely we have found that for a properly working comagnetometer, it is required that both the nuclear spin polarization and the alkali atomic spin lifetime are relatively small so that their product remains below a critical value which depends on the specific magnetic moment of the alkali spin in use. However, for the merit of the comagnetometer signal, a strong nuclear spin magnetization is needed. This intrinsic conflict ultimately sets the limit of the comagnetometry response signal for a given trispin system as we will see below.

By analyzing the case of underdamping more in detail, we can see that the presence of high-frequency oscillations prevents the alkali atomic spin motion from smoothly and adiabatically following the nuclear spin precession. In particular, if we decompose the overall evolution of alkali spins into a fast oscillation and an adiabatic slow oscillation, the fact that the fast oscillation and the adiabatic slow motion are not in phase leads to two main effects:

(1) the phase of the overall oscillation is effectively advanced or retarded in a continuous way;

(2) the amplitude of the overall oscillation is reduced by different amounts, depending on the local phase relation.

The first effect leads to a continuous phase accumulation and eventually generates a frequency shift. This is shown in the Fourier spectral analysis of Fig. 2 by the side modes appearing around the nuclear spin Larmor frequency (and associated peaks as explained in Ref. [8]). The second effect leads to a reduction of the oscillation amplitude at the nuclear spin Larmor frequencies as $\lambda M_0^n T^e$ increases (two highest peaks around 6 and 16 Hz of the dashed red line versus the solid blue line in Fig. 2). As a combined result, the NMR peaks at the nuclear spin Larmor frequencies become broader and lower in amplitude. This makes the overall spectral resolution worse, which, in turn, degrades the comagnetometer performances.

In a classical driven harmonic oscillator with a small damping, a resonance amplification is possible when the natural frequency approaches the driving frequency. This also happens in the trispin system, however, in this case the overdamping condition cannot be realized, and the NMR spectra become crowded with side mode components (similar to the dashed red line in Fig. 2). Ultimately, the original ^{3}He and ^{129}Xe resonance peaks, shown in our simulations, will be
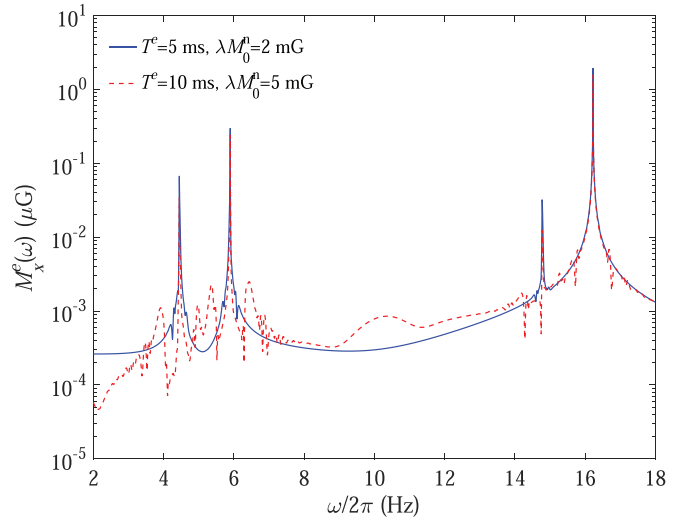

FIG. 2. Fourier transformation spectra for simulated 200-s oscillation of alkali atomic spin transverse magnetization. The spectra is shown as a function of initial nuclear spin magnetization M_0^n and alkali atomic spin lifetime T^e. Extra side modes emerge near the main peaks as M_0^n and T^e increase, proving the gradual phase and frequency shift effects as a result of the under damping alkali atomic spin oscillations. The main resonance peaks are located at 5.89 and 16.22 Hz, determined by the ^{129}Xe and ^{3}He atomic gyromagnetic ratios ($\gamma_{\text{Xe}} = 2\pi \times 1.178$ kHz/G, $\gamma_{\text{He}} = 2\pi \times 3.244$ kHz/G) and bias magnetic-field $B_0 = 5$ mG.

fully immersed in noise and not distinguishable anymore. The system, in that case, becomes clearly unsuitable for high precision comagnetometer or gyroscope applications, and we will not consider this scenario any further.

For practical purposes, we now discuss the maximum attainable comagnetometer response. First, as we have explained above, this should be estimated in the linear-response range, i.e., in the overdamping region where the alkali atomic spin follows the nuclear spin precession adiabatically. Second, the response is proportional to both the nuclear spin magnetization and the alkali atomic spin lifetime so that they will be as high as possible. These two conditions determine the maximal comagnetometer response.

To find out this maximum response, we simulated the alkali atomic spin evolution for 200 s in the time domain, and then we performed a Fourier transform to extract the peak value at the ^{3}He Larmor frequency. We repeated the process for different values of the nuclear spin magnetization and the alkali atomic spin lifetime. Finally, we plotted the comagnetometry signal amplitude as a function of the λM_0^n spanning a range of three orders of magnitude at different T^e's as shown in Fig. 3.

A single maximum response signal is found as a function of the nuclear spin magnetization for different alkali atomic spin lifetimes. One can also see that when the alkali atomic spin lifetime is short, the response signal reaches the maximum at high nuclear spin magnetization, and vice versa. These results are in agreement with our previous analysis. The maximum response is almost constant over a range of two orders of magnitude for nuclear magnetization from 0.1 to 10 mG and over a range of two orders of magnitude for alkali atomic spin lifetime from 0.04 to 5 ms. This means that the system has
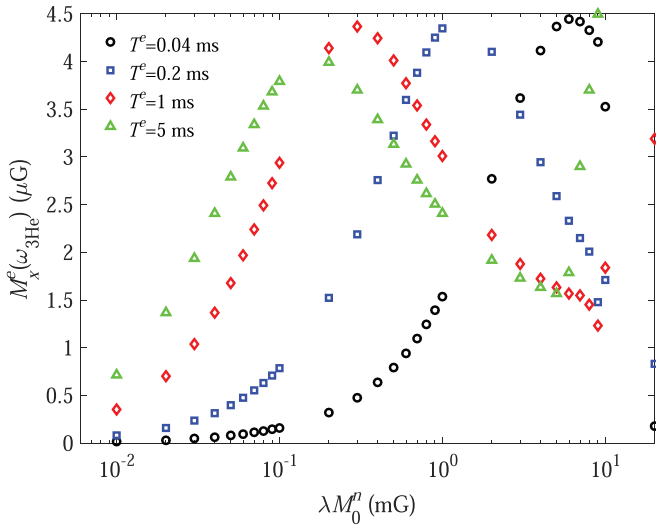
FIG. 3. The comagnetometer response M_x^e at ^{3}He spin precession Larmor frequency as a function of nuclear spin magnetization M^n at various alkali atomic spin lifetimes T^e. A maximum response can be obtained over a large range, almost two orders of magnitude for both M^n and T^e parameters. The abnormal increasing response of the last few points (two red squares and four green triangles) at high M^n for $T^e = 1$ and 5 ms are region where the resonance amplification happens for small damping and strong driving.

a relatively large linear-response regime. Fortunately, these ranges can be easily covered experimentally by tuning parameters, such as the temperature and the buffer gas pressure. It is also interesting to note that the best current experimental values, reported, e.g., in Refs. [3,7], fall within the best region of parameter highlighted by our simulations.

In addition, the response signal is a cross product of the alkali atomic spin magnetization $\mathbf{M}^e$ and noble-gas nuclear spin magnetization $\mathbf{M}^n$, which means it is also proportional to the alkali atomic spin magnetization. Given a certain initial alkali spin magnetization M_0^e, the existence of the maximum response signal indicates that there is an upper limit for the comagnetometer output based on the alkali-metal–noble-

gas hybrid spin system. Considering the critical damping condition of Eq. (4), the maximum response of the trispin comagnetometer is determined only by the alkali atomic spin parameters, i.e., by the spin magnetization and lifetime of the alkali atom gas.

Finally, we point out that the trispin system dynamics converges even in the presence of a multiple peak spectral structure, observed for some specific conditions in Refs. [3,8]. Even if a chaotic relaxation might not be excluded in these cases (see, for example, Refs. [18,19] and references therein) from our numerical analysis this appears not to have a major impact on the significance of the critical damping condition and on the main results outlined in the present paper.

In conclusion, we have investigated the intrinsic response dynamics of a comagnetometer based on a gaseous alkali-metal–noble-gas hybrid trispin system. From the perspective of a damped harmonic oscillator, we revealed the important relations between the key atomic spin parameters. The alkali atomic spin oscillator has to work at the overdamping condition, i.e., a relative low noble-gas nuclear spin magnetization and short alkali atomic spin lifetime, to have a linear-response and achieve the maximum signal. The overdamping can also serve as a possible mechanism for coherence transfer between the alkali atomic spin and noble-gas nuclear spins.

For the benefit of a high performance comagnetometer or NMR gyroscope, counterintuitively, a compromise between strong noble-gas nuclear spin magnetization and long alkali atomic spin lifetime will be made. For future experiments on trispin NMR gyroscopes, a maximum achievable response is given as a function of the noble-gas nuclear spin magnetization and alkali atomic spin lifetime. The limit is inherent in the response dynamics of the hybrid trispin system. We stress that, even though we used the ^{87}Rb-^{3}He-^{129}Xe system for our simulations, the theoretical results obtained here are valid for any alkali-metal–noble-gas hybrid trispin system.

[1] T. G. Walker and W. Happer, Spin-exchange optical pumping of noble-gas nuclei, Rev. Mod. Phys. **69**, 629 (1997).

[2] M. Bulatowicz, R. Griffith, M. Larsen, J. Mirijanian, C. B. Fu, E. Smith, W. M. Snow, H. Yan, and T. G. Walker, Laboratory Search for a Long-Range *t*-Odd, *p*-Odd Interaction from Axion-like Particles Using Dual-Species Nuclear Magnetic Resonance with Polarized ^{129}Xe and ^{131}Xe Gas, Phys. Rev. Lett. **111**, 102001 (2013).

[3] M. E. Limes, D. Sheng, and M. V. Romalis, ^{3}He−^{129}Xe Comagnetometery using ^{87}Rb Detection and Decoupling, Phys. Rev. Lett. **120**, 033401 (2018).

[4] E. A. Donley, Nuclear magnetic resonance gyroscopes, *SENSORS, 2010* (IEEE, 2010), pp. 17–22.

[5] T. G. Walker and M. S. Larsen, Spin-exchange-pumped NMR gyros, Adv. At. Mol. Opt. Phys. **65**, 373 (2016).

[6] T. W. Kornack and M. V. Romalis, Dynamics of Two Overlapping Spin Ensembles Interacting by Spin Exchange, Phys. Rev. Lett. **89**, 253002 (2002).

[7] A. Korver, D. Thrasher, M. Bulatowicz, and T. G. Walker, Synchronous Spin-Exchange Optical Pumping, Phys. Rev. Lett. **115**, 253001 (2015).

[8] G. Liu, Trispin dynamics in an alkali-metal–noble-gas nuclear-magnetic-resonance gyroscope, Phys. Rev. A **99**, 033409 (2019).

[9] S. R. Schaefer, G. D. Cates, T.-R. Chien, D. Gonatas, W. Happer, and T. G. Walker, Frequency shifts of the magnetic-resonance spectrum of mixtures of nuclear spin-polarized noble gases and vapors of spin-polarized alkali-metal atoms, Phys. Rev. A **39**, 5613 (1989).

[10] M. V. Romalis and G. D. Cates, Accurate ^{3}He polarimetry using the Rb Zeeman frequency shift due to the

Rb−^{3}He spin-exchange collisions, Phys. Rev. A **58**, 3004 (1998).

[11] J. C. Allred, R. N. Lyman, T. W. Kornack, and M. V. Romalis, High-Sensitivity Atomic Magnetometer Unaffected by Spin-Exchange Relaxation, Phys. Rev. Lett. **89**, 130801 (2002).

[12] Z. L. Ma, E. G. Sorte, and B. Saam, Collisional ^{3}He and ^{129}Xe Frequency Shifts in Rb–Noble-Gas Mixtures, Phys. Rev. Lett. **106**, 193005 (2011).

[13] M. E. Limes, N. Dural, M. V. Romalis, E. L. Foley, T. W. Kornack, A. Nelson, L. R. Grisham, and J. Vaara, Dipolar and scalar ^{3}He−^{129}Xe frequency shifts in stemless cells, Phys. Rev. A **100**, 010501(R) (2019).

[14] J. Vaara and M. V. Romalis, Calculation of scalar nuclear spin-spin coupling in a noble-gas mixture, Phys. Rev. A **99**, 060501(R) (2019).

[15] S. Haroche and C. Cohen-Tannoudji, Resonant Transfer of Coherence in Nonzero Magnetic Field Between Atomic Levels of Different *g* Factors, Phys. Rev. Lett. **24**, 974 (1970).

[16] R. Konrat, I. Burghardt, and G. Bodenhausen, Coherence transfer in nuclear magnetic resonance by selective homonuclear Hartmann-Hahn correlation spectroscopy, J. Am. Chem. Soc. **113**, 9135 (1991).

[17] O. Katz, O. Peleg, and O. Firstenberg, Coherent Coupling of Alkali Atoms by Random Collisions, Phys. Rev. Lett. **115**, 113003 (2015).

[18] R. Venegeroles, Leading Pollicott-Ruelle resonances for chaotic area-preserving maps, Phys. Rev. E **77**, 027201 (2008).

[19] R. Wiebe and L. Virgin, A heuristic method for identifying chaos from frequency content, Chaos **22**, 013136 (2012).